Synthesis and Characterization of Outer Sphere−Outer Sphere Connected Organoplatinum Dendritic Networks from Surface-Difunctionalized and Surface-Trifunctionalized Dendritic Monomers

Hak-Fun Chow* and Cham-Fai Leung

Department of Chemistry, The Chinese University of Hong Kong, Shatin, NT, Hong Kong SAR

Luan Xi and Leo W. M. Lau

Department of Physics, The Chinese University of Hong Kong, Shatin, NT, Hong Kong SAR

Received October 15, 2003; Revised Manuscript Received February 27, 2004

ABSTRACT: Two different approaches toward the syntheses of cross-linked dendritic networks from surface-functionalized polyether dendritic monomers were reported. The first series (type I) of dendritic networks (G1−G3) was prepared by a 3:2 copolymerization of surface bifunctionalized (G1−G3) dendritic monomers having two reactive arylethynyl surface groups with a small size trifunctional organoplatinum branching monomer {tris[*trans*-chlorobis(triethylphosphine)platinum]mesitylene-2,4,6-triethynylene} containing three reactive chloroplatinum functionalities. Facile network formation was realized for the G1 dendritic monomer, while linear, nonbranching dendritic polymers were predominately produced from the higher generation G2 and G3 monomers. The second series (type II) of dendritic networks (G0−G2) was prepared by a 3:2 copolymerization of a small size bifunctional organoplatinum monomer {bis[*trans*-chlorobis(triethylphosphine)platinum]-4,4′-biphenylene-1,1′-diethynylene} having two reactive chloroplatinum moieties with surface-trifunctionalized (G0−G2) dendritic branching monomers with three reactive arylethynyl surface groups. Highly cross-linked dendritic networks were formed in all three generation of dendritic monomers. The structures of the soluble, linear dendritic polymers and the insoluble dendritic networks were characterized by nuclear magnetic resonance spectroscopy, gel permeation chromatography, scanning electron microscopy, scanning tunneling microscopy and/or energy-dispersive X-ray spectroscopy. The difference in the copolymerization behavior between these two approaches was rationalized in terms of steric inhibition during cross-linking in the type I dendritic network architecture.

1. Introduction

The use of simple dendritic subunits as basic building blocks toward the construction of higher order, complex dendritic networks has become a topic of current interest.[1] Depending on the mode of subunit connections, dendritic networks can be subdivided into inner sphere−inner sphere, inner sphere−outer sphere and outer sphere−outer sphere connected systems. Thus far most research efforts conducted in this area have been focused on inner sphere−inner sphere connected dendronized polymers.[2] These polymers are prepared via the interconnection of dendron subunits via their reactive focal point functional groups. One of the interesting aspects of dendronized polymers lies in their unique structural features. For examples, some of them adopt cylindrical geometries[2] while others self-assemble into spherical structures.[3] The ability to control the molecular conformation of polymers and to prepare shape-controlled macromolecules of nanoscopic scales are of great importance to polymer science. Materials such as these possessing highly ordered internal architecture are of enormous potential in catalysis and nanotechnology applications.

The other two modes of dendrimer connection, namely inner sphere−outer sphere[4] and outer sphere−outer sphere connections,[5] however, are less studied. Between these two, the latter connection strategy appears more appealing because the reactive connecting groups are now located on the dendrimer surface and therefore their reactivity should be less influenced by steric inhibition during network formation. We recently reported the first syntheses of dendritic necklaces[6] **1** by the controlled copolymerization of bis(ethynyl) surface-functionalized polyether dendrimers **2** and *trans*-[$(Et_3P)_2$-$PtCl_2$] using a new outer sphere−outer sphere connection strategy (Scheme 1).[7] Depending on the size or generation of the dendritic beads **2**, dendritic necklaces **1** with degree of polymerization (DP_w) ranging from 30 to 880 could be readily prepared. These values were comparable to the high-end DP_w values of dendronized polymers[2] prepared from the inner sphere−inner sphere connection protocol.

Scheme 1. Synthesis of "Dendritic Necklaces" 1 by an Outer Sphere−Outer Sphere Connection Strategy

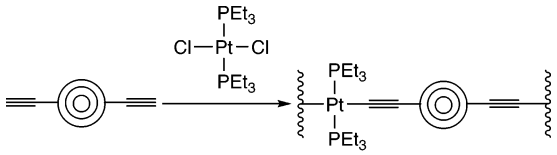

Having demonstrated that the outer sphere−outer sphere connection strategy was a viable method for the construction of high molecular weight linear dendritic necklaces **1**, we then examined the possibility of constructing highly cross-linking dendritic networks using a similar approach.[8] Two different construction protocols

* Corresponding author. Telephone: +852 26096341. Fax: +852 26035057. E-mail: hfchow@cuhk.edu.hk.

10.1021/ma035548f CCC: $27.50
Published on Web 04/15/2004

Scheme 2. Formation of (a) Type I and (b) Type II Dendritic Networks

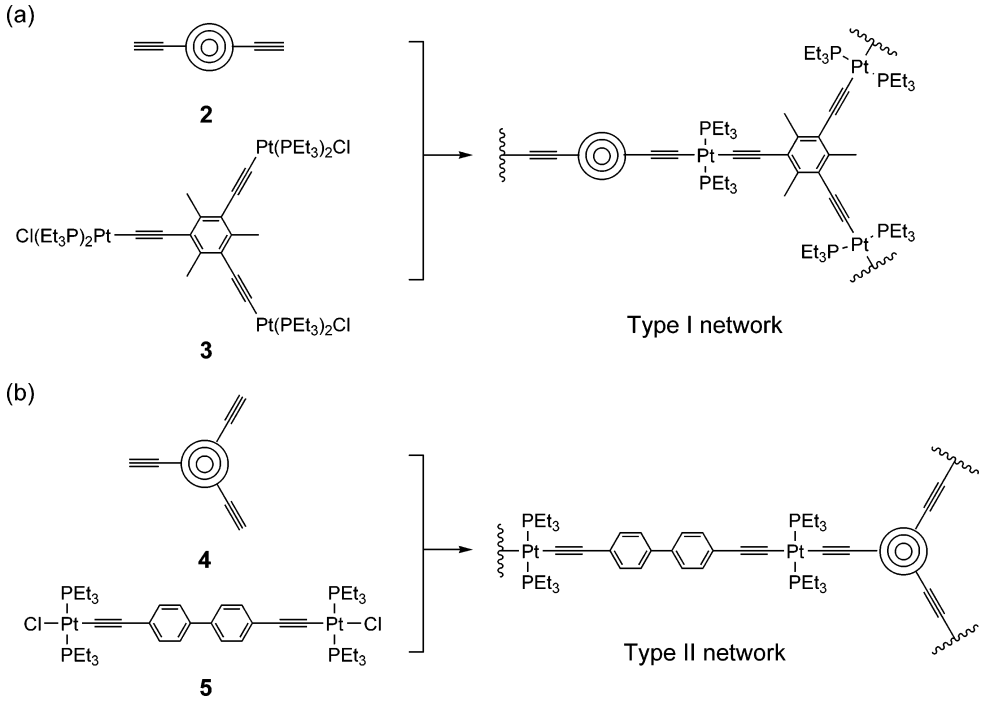

are reported in this paper. The first type of dendritic networks (named type I network hereafter) was prepared by a 3:2 copolymerization of the previously mentioned surface bifunctionalized dendritic monomers **2** with a small size trifunctional organoplatinum brancher **3** (Scheme 2a). In this method the three reactive surface chloroplatinum groups of the branching monomer **3** are in close proximity to each other. The second series of networks (type II) was synthesized by a 2:3 copolymerization of a new series of surface-trifunctionalized polyether dendritic branching monomers **4** with a small bifunctional organoplatinum complex **5** (Scheme 2b). In contrast to the first strategy, the three reactive surface ethynyl groups are now placed at the extreme ends of three separate dendrons in the branching monomer **4**. In contrast to polymer networks formed from small molecular size polyfunctional monomers, we found that efficient dendritic network formation strongly depended on the molecular size of the dendritic monomers as well as on the spatial separation of the reactive surface functional groups of the trifunctional brancher. Such new findings therefore provide useful guidelines toward the future synthetic design of highly cross-linking dendritic network systems.

2. Results and Discussion

2.1. Type I Dendritic Networks. 2.1.1. Synthesis. The bifunctional dendrimers **2** of different generations chosen for the preparation of the type I dendritic networks were bis(ethynyl) surface-functionalized G1−G3 dendrimers **6**−**8**[6] (Scheme 3). Their structural skeletons were based on a hydroquinone central core and 3-(3,5-dihydroxyphenylpropoxy) branching units. Furthermore, two arylethynyl units were employed as the "reactive" surface groups while 4-*tert*-butylphenoxy moieties were used as the "inert" surface groups. Copolymerizations of the various surface bifunctionalized dendrimers **6**−**8** with the trifunctional organoplatinum complex **3**[9] (0.67 equiv) were conducted under N_2 atmosphere in the presence of a catalytic amount of CuI in a 1:1 mixture of CH_2Cl_2 and *i*-Pr_2NH at 25 °C for 6−12 h. A polymer gel **9** was formed from the copolymerization of the G1 dendritic monomer **6** and complex **3**. The G1 dendritic network **9** so obtained after purification was a yellow solid that was insoluble in organic solvents.

In contrast, no gel formed in the copolymerizations of the G2 **7** or G3 dendrimers **8** with the triplatinum species **3** under similar conditions. The resulting G2 **10** and G3 dendritic networks **11** were isolated as yellow solids from precipitation of the crude product in acetone. The yellow solids can be redissolved in organic solvents such as CH_2Cl_2 and THF.

2.1.2. Characterization. The fact that the type I G1 dendritic network **9** formed from the smallest G1 dendritic monomer **6** was insoluble suggested that it had a highly cross-linking architecture. Unfortunately, its insolubility in organic solvents precluded its structural identification by solution methods such as nuclear magnetic resonance (NMR), size exclusion chromatography (SEC), and laser light scattering techniques. On the other hand, the higher generation type I G2 **10** and G3 **11** dendritic networks were expected to have a lesser degree of cross-linking because of their good solubility. Examination of the ^1H NMR spectra of the soluble networks **10** and **11** revealed an upfield shift of the aromatic protons (δ 7.4 → 7.2; δ 6.9 → 6.7, relative to the corresponding dendritic monomers **7** and **8**) due to the arylethynyl surface groups, together with the disappearance of the acetylenic signals at δ 3.0 (Figure 1). Hence, all the surface ethynyl moieties were complexed to the platinum metals. The methyl proton signal (δ 2.57) due to triplatinum brancher and those of the triethylphosphine ligands (δ 1.2) could also be identified.

For a perfectly branched structure, the molar ratio of the bifunctional dendrimer **2** to the triplatinum unit **3** is 3:2. Hence, the theoretical relative integration (2 × 9 units) of the methyl signal (δ 2.57) due to the triplatinum brancher relative to that (3 × 18 units) of the aromatic hydrogens (δ 6.28−6.38) of the 3-(3,5-

Scheme 3[a]

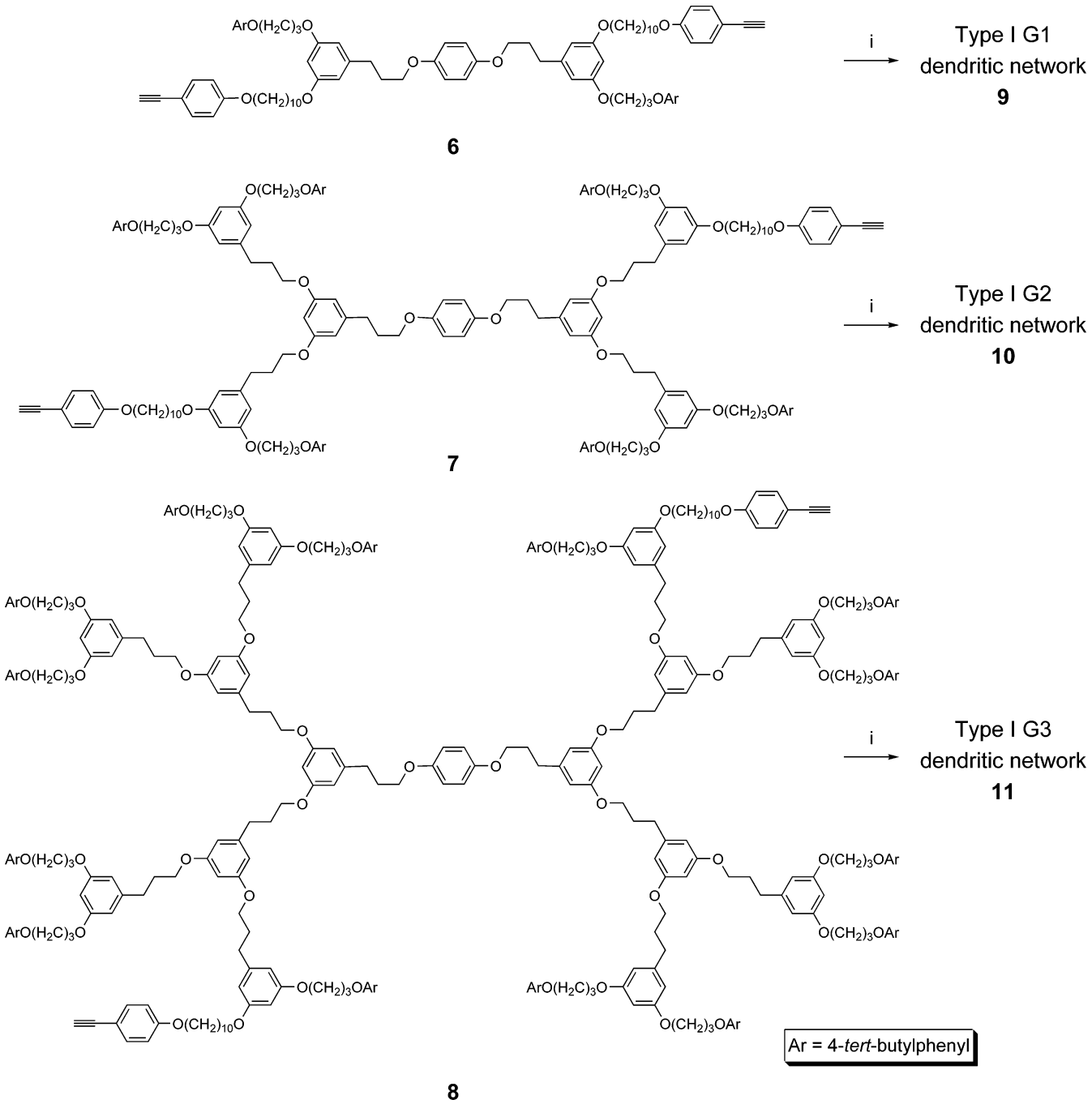

[a] Reagents and conditions: (i) **3** ($^2/_3$ equiv), CuI (catalytic), CH_2Cl_2/*i*-Pr_2NH (1:1), 25 °C, 6−12 h.

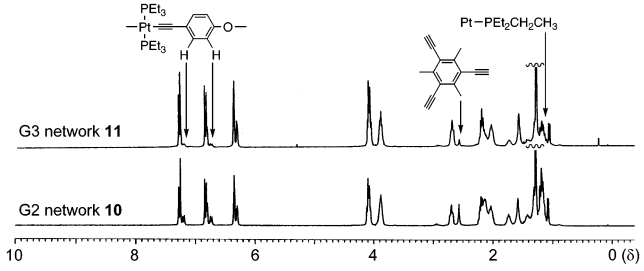

Figure 1. ^{1}H (300 MHz, $CDCl_3$) nuclear magnetic resonance spectra of the soluble type I G2 **10** and G3 **11** dendritic networks.

dihydroxyphenyl)propoxy branching units of a perfectly branched dendritic network should be 18:54. On examination of the ^{1}H NMR spectrum of the G2 dendritic network **10**, the experimentally measured relative integration values of the two relevant signals were 24:54, indicating that the % content of the bifunctional dendrimer was in excess in this type I G2 structure. On the other hand, the relative integration of the above-mentioned signals due to a linear, nonbranching dendritic necklace (Figure 2) formed from a 1:1 copolymerization of the G2 monomer **7** and the platinum complex **3** should be 27:54. On the basis of the experimental values, one can conclude that the G2 "dendritic network" has a structure that is closer to a linear dendritic necklace architecture with relatively little branching at the triplatinum branching centers. Examination of the ^{31}P{^{1}H} NMR spectrum of compound **10** revealed several sets of signals at δ 10−25, indicating the presence of more than one kind of phosphorus atoms

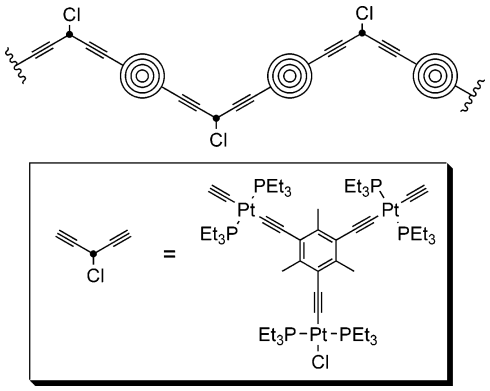

Figure 2. Linear, end-linking dendritic necklace formed from the 1:1 copolymerization of a surface bifunctionalized dendrimer (**7** or **8**) with trifunctional platinum complex **3** with no cross-linking.

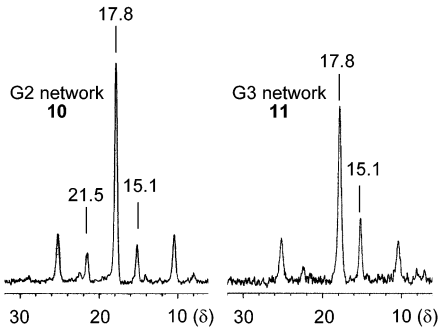

Figure 3. $^{31}P\{^{1}H\}$ (161.9 MHz, $CDCl_3$) nuclear magnetic resonance spectra of soluble type I G2 **10** and G3 **11** dendritic networks.

Table 1. Size Exclusion Chromatography (SEC) Data of Soluble G2 10 and G3 11 Dendritic Networks[a]

dendritic network	M_w[b] $\times 10^{-3}$ (g/mol)	PDI[c]	DP_w[d]
G2 **10**	79	2.1	19
G3 **11**	48	1.7	7

[a] Columns: Waters Styragel columns HR 1, HR 2, HR 3, and HR 4 in series. Solvent: THF (flow rate = 1.0 mL/min). Temperature: 40 °C. Calibration standards: polystyrenes. [b] M_w = weight-average molecular weight. [c] PDI = polydispersity index M_w/M_n. [d] DP_w = degree of polymerization, calculated based on M_w values obtained from SEC data.

in the structure (Figure 3). The major set of signal was found to locate at δ 17.8, and was accompanied by two ^{195}Pt satellite peaks ($^{1}J_{Pt-P} \sim 2390$ Hz) of one-sixth intensity. The chemical shift value was similar to those of the dendritic necklaces reported earlier[6] and this signal was attributed to the phosphorus nuclei adjacent to the bis(alkynyl) platinum centers (i.e., C≡C−Pt−C≡C). Two minor sets of ^{31}P signals (δ 15.1 and 21.5) were also observed and were most likely due to the phosphorus nuclei adjacent to the unreacted chloroplatinum centers (i.e. C≡C−Pt−Cl) located inside the polymer chain and at the chain ends. Similar spectral features were also noted for the G3 dendritic network **11**, although in this case the intensity of the minor signal at δ 21.5 was weaker, while the one at δ 15.1 became more prominent.

The soluble networks **10** and **11** were subjected to SEC analysis and the SEC estimated molecular weights (M_w), based on polystyrene standards, were tabulated (Table 1). The polydispersity index (PDI) values (~2) obtained were comparable to those of the dendritic necklaces **1**[6] reported by us, although the DP_w (7−19)

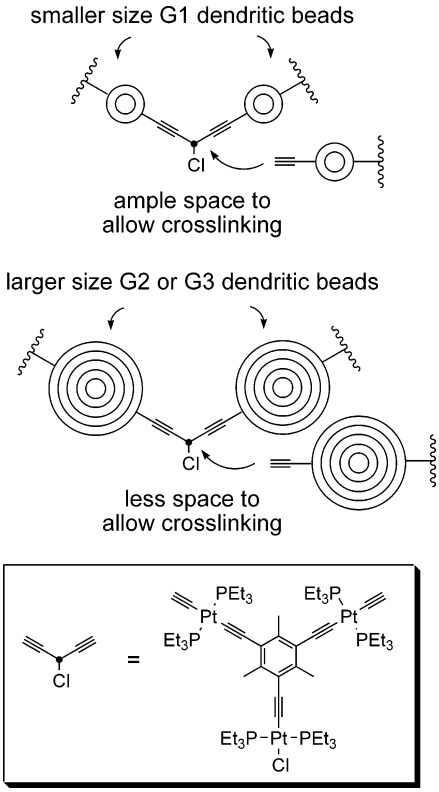

Figure 4. Formation of cross-linking dendritic networks.

values were significantly lower. The M_w value of the G2 network was slightly greater than that of the G3 network, suggesting that the smaller size G2 dendritic monomer **7** was more effective than the G3 analogue **8** toward polymerization. Hence, it was clear that steric factor played a very important role in disfavoring the copolymerization of surface bifunctionalized dendrimers with the small size trifunctional monomer **3**.

The question remained to be answered was why only the smallest G1 monomer **6** afforded a highly cross-linking gel under similar polymerization conditions. It was noted that cross-linking invariably involved the placement of three dendritic subunits on a trifunctional organoplatinum branching point. Because of the relatively small size of the platinum branching unit **3**, the distance between the bulky dendritic subunits was very short and hence the steric environment in the vicinity of the branching point must be highly congested. As a result, steric repulsion must develop during entry of the third dendritic species during cross-linking (Figure 4). This repulsion should be more prominent if the size of the dendritic monomer is large, i.e. higher generation dendritic beads (such as G2 and G3 in our case) should disfavor the formation of cross-linked networks. On the other hand, steric congestion near the organoplatinum brancher was less severe for the smallest size G1 monomer and therefore a cross-linked network was formed.

Thus far the structural identity of the G1 network **9** has evaded proper characterization due to its insolubility property. Hence, energy-dispersive X-ray (EDX) spectroscopy was employed to determine the elemental compositions of the intractable G1 network. Because of the presence of a thin layer of gold coating during sample treatment, the signal originated from the Pt atoms was partially masked by that of the Au atoms and hence the accuracy of the measured % Pt content

Table 2. Energy-Dispersive X-ray (EDX) Analysis Results of Type I Dendritic Networks 9−11

dendritic network	elemental content (%)[a]		
	Pt	C	P
G1 **9**	19.7 (17.0, 20.7)	59.5 (62.9, 58.3)	6.9 (5.4, 6.6)
G2 **10**	22.4 (10.7, 14.0)	65.0 (68.4, 64.6)	7.1 (3.4, 4.4)
G3 **11**	8.5 (6.1, 8.4)	78.7 (72.1, 69.5)	2.9 (1.9, 2.7)

[a] First and second values in parentheses are theoretical values calculated from molecular structures with perfect branching pattern and from 1:1 linear structures without branching, respectively.

Figure 5. Scanning electron microscopy image (dried gel) of type I G1 dendritic network **9** (left: 100 μm × 100 μm) and scanning tunneling microscopy images (spin-cast samples) of type I G2 **10** (middle: 82 nm × 82 nm) and type I G3 **11** dendritic networks (right: 220 nm × 220 nm) on highly orientated pyrolytic graphite (HOPG).

had a high degree of uncertainty (Table 2). Nonetheless, the measured values are in good agreement with their elemental compositions in all three type I dendritic networks **9**−**11**.

The morphologies of the dendritic networks were examined by scanning electron microscopy (SEM) and scanning tunneling microscopy (STM) (Figure 5). The SEM image of the type I G1 dried gel showed a dense structure that was typical of a network architecture. On the other hand, spin-cast samples of the soluble type I G2 and G3 networks on highly orientated pyrolytic graphite (HOPG) revealed the presence of either clusters or linear, chainlike structures. Generally, chains were more frequently observed than clusters and many of them could extend over 200 nm long. Most G2 chains have cross-sectional diameters in the regions of 4−11 nm while those of the G3 chains have diameters in the region of 7−14 nm. These values are much bigger than that expected for a single dendritic necklace chain, suggesting that they are chain bundles formed from the inter-winding of individual necklaces.

2.2. Type II Dendritic Networks. The failure to create highly cross-linking type I G2 and G3 dendritic networks by the copolymerization of surface bifunctionalized dendrimers **7**−**8** and the small triplatinum comonomer **3** prompted us to reexamine the network formation strategy. We envisage that steric hindrance can be eliminated if a much bigger size trifunctional brancher is used in the copolymerization. One strategy is to put the three reactive groups on the surface of a dendrimer and use the resulting surface-trifunctionalized dendrimer as a brancher in the copolymerization with a bifunctional platinum complex. The much larger size of a dendritic molecule now guarantees that the reactive surface groups are far apart from each other and the formation of a cross-linking network should be facilitated due to a relief of steric hindrance at the branching points.

2.2.1. Synthesis of Surface-Trifunctionalized Dendritic Monomers 12—14. The structures of the surface-trifunctionalized G0−G2 dendrimers **12**−**14** are shown in Figure 6. They were constructed based on a 1,1,1-tris(4-hydroxyphenyl)ethane central core, 3-(3,5-dihydroxyphenyl)propoxy branching units, 3-(4-*tert*-butylphenoxy)propoxy inert surface groups and three 10-[(4-ethynyl)phenoxy]decoxy reactive surface groups. Similar to the bifunctional dendritic monomers **6**−**8** used in the preparation of type I dendritic networks, the reactive ethynyl groups are also located at the end of three separate C-10 chains to eliminate possible steric interactions during copolymerization.

To avoid complications that might arise during synthetic transformations, the three labile arylethynyl surface groups were initially masked as the corresponding aryl iodide functionalities. The synthesis of the G0 trifunctional dendrimer **12** involved a direct coupling of 3.2 equiv of a previously reported iodine-containing G0 bromide dendron[6] **15** to 1,1,1-tris(4-hydroxyphenyl)-ethane (**16**) in the presence of Cs_2CO_3 and dibenzo-24-crown-8 (Scheme 4). The triiodide G0 dendrimer **17** was then converted to the corresponding tris(trimethylsilylethynyl) derivative **18** via Sonogashira coupling[10] with trimethylsilylacetylene. Subsequent deprotection of the trimethylsilyl groups under basic conditions (K_2CO_3, methanol) then afforded the target dendrimer **12** in 23% overall yield from the G0 dendron **15**.

In a similar manner, coupling of 3.2 equiv of the unsymmetrical G1 **19** and G2 **20** bromide dendrons[6] with the same central core **16** produced the corresponding G1 **21** and G2 **22** dendrimers, respectively (Scheme 5). The aryl iodide dendrimers **21** and **22** were then transformed to the corresponding aryltrimethylsilylacetylene dendrimers **23** and **24**, respectively, via the Sonogashira coupling with trimethylsilylacetylene. Subsequent removal of the trimethylsilyl groups then gave the target tris(ethynyl) surface-functionalized dendritic monomers **13** and **14** in 27% and 20% overall yield from dendrons **19** and **20**, respectively.

The bifunctional platinum complex **5** was prepared as a yellow solid in 51% yield by treatment of 1,1′-bis-(ethynyl)-4,4′-biphenyl[10] with 2.2 equiv of *trans*-[Pt-$(PEt_3)_2Cl_2$] in the presence of CuCl and *i*-Pr_2NH.

2.2.2. Synthesis of Type II Dendritic Networks. Copolymerizations of the various surface-trifunctionalized dendrimers **12**−**14** and the bifunctional platinum complex **5** (1.5 equiv) were performed in the presence of CuCl and *i*-Pr_2NH under N_2 atmosphere to furnish the type II G0−G2 dendritic networks **25**−**27**, respectively (Scheme 6). Gelation of the reaction mixture began to occur when the reaction was stand at 25 °C after 15 min. The formation of insoluble polymer gels with all three generation of dendritic monomers suggested that this alternative strategy indeed afforded dendritic networks with extensive cross-linking. Hence, this experiment provided strong evidence that steric inhibition was not significant during network cross-linking when the reactive surface ethynyl functional groups on the branching monomers were far apart. The resulting dendritic polymer gels were not soluble in organic solvents even after prolonged heating and stirring in organic solvents.

2.2.3. Characterization. The structure of the surface bifunctionalized dendritic monomers **12**−**14** and their precursor molecules were readily confirmed by ^1H and ^{13}C NMR spectroscopy. For the three triiodo surface-functionalized derivatives **17**, **21**, and **22**, the aromatic protons due to the aryl iodide moieties resonated at δ 7.53 and 6.66, while those of the central core unit resonated at δ 6.98 and 6.77. On the other hand, the

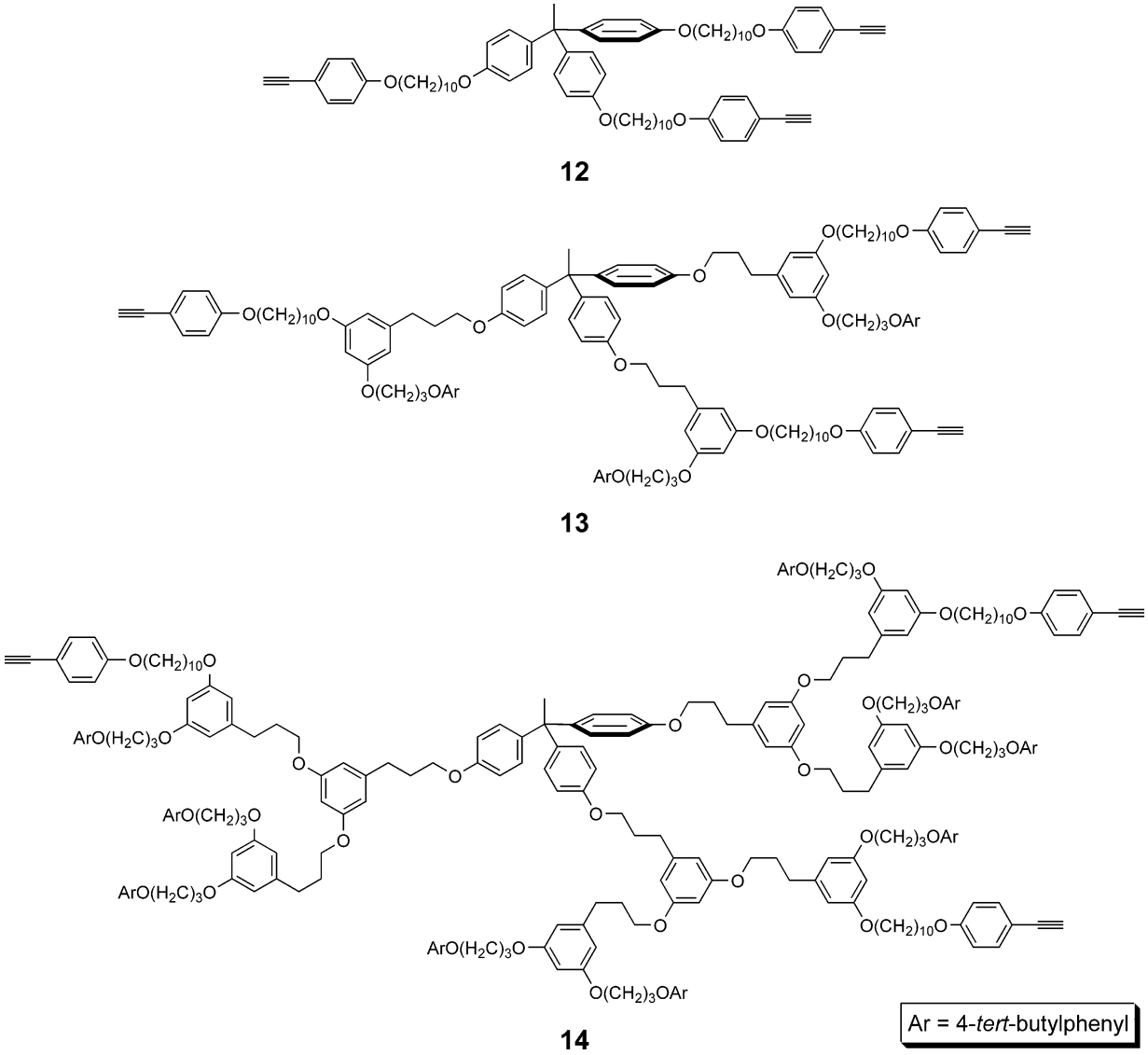

Figure 6. Structures of surface-trifunctionalized dendritic monomers **12**−**14**.

Scheme 4[a]

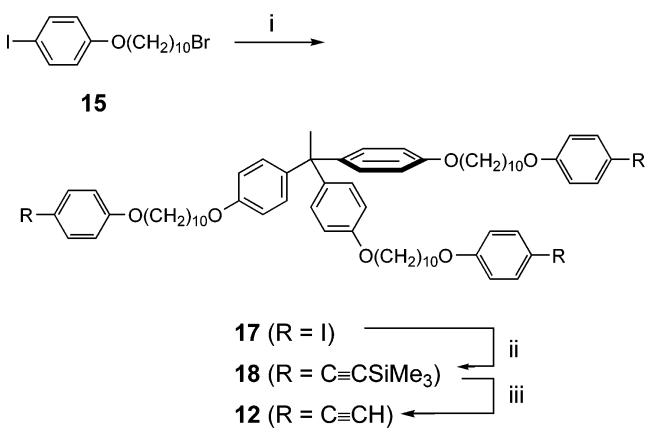

[a] Reagents and conditions: (i) 1,1,1-tris(4-hydroxyphenyl)ethane (**16**) (0.31 equiv), Cs_2CO_3, dibenzo-24-crown-8, DMF, 110 °C, 2 h; (ii) $(CH_3)_3SiC{\equiv}CH$, $Pd(PPh_3)_2Cl_2$, CuI, PPh_3, NEt_3, toluene, 60 °C, 6 h; (iii) K_2CO_3, MeOH, THF, 25 °C, 1.5 h.

aromatic ^{1}H NMR signals of the "inert" *tert*-butylphenoxy groups were found to be located at δ 7.29 and 6.84 for the G1 **21** and G2 **22** compounds. The methyl signal due to the central core unit, which resonated as a singlet at δ 2.10 for the G0 **17** compound, was obscured by other signals for the G1 **21** and G2 **22** dendrimers.

The trimethylsilylethynyl derivatives **18**, **23**, and **24**, on the other hand, each exhibited a sharp singlet at δ 0.23 due to the trimethylsilyl signals. The ^{1}H NMR signals of the aromatic protons of the surface aryltrimethylsilylethyne units were shifted to δ 7.38 and 6.80, while the resonance positions of all other protons remained essentially unchanged.

With regard to the structure of the tris(ethynyl) monomers **12**−**14**, their respective ^{1}H NMR spectra showed a sharp singlet signal located at δ 2.98 due to the terminal acetylenic protons and a set of aromatic AB signals located at δ 7.40 and δ 6.83 due to the aromatic protons of the "reactive" surface arylethynyl functionalities (Figure 7). The set of aromatic AB system due to the "inert" surface groups was also found at δ 7.29 and 6.84 for the G1 **13** and G2 **14** compounds. The methyl proton signal at δ 2.10 and those of the aromatic protons (δ 6.97 and δ 6.77) of the central core could also be identified. Furthermore, the relative integration of the acetylenic signal was noted to decrease with respect to that of the surface *tert*-butyl signal with increasing dendrimer generation.

Scheme 5[a]

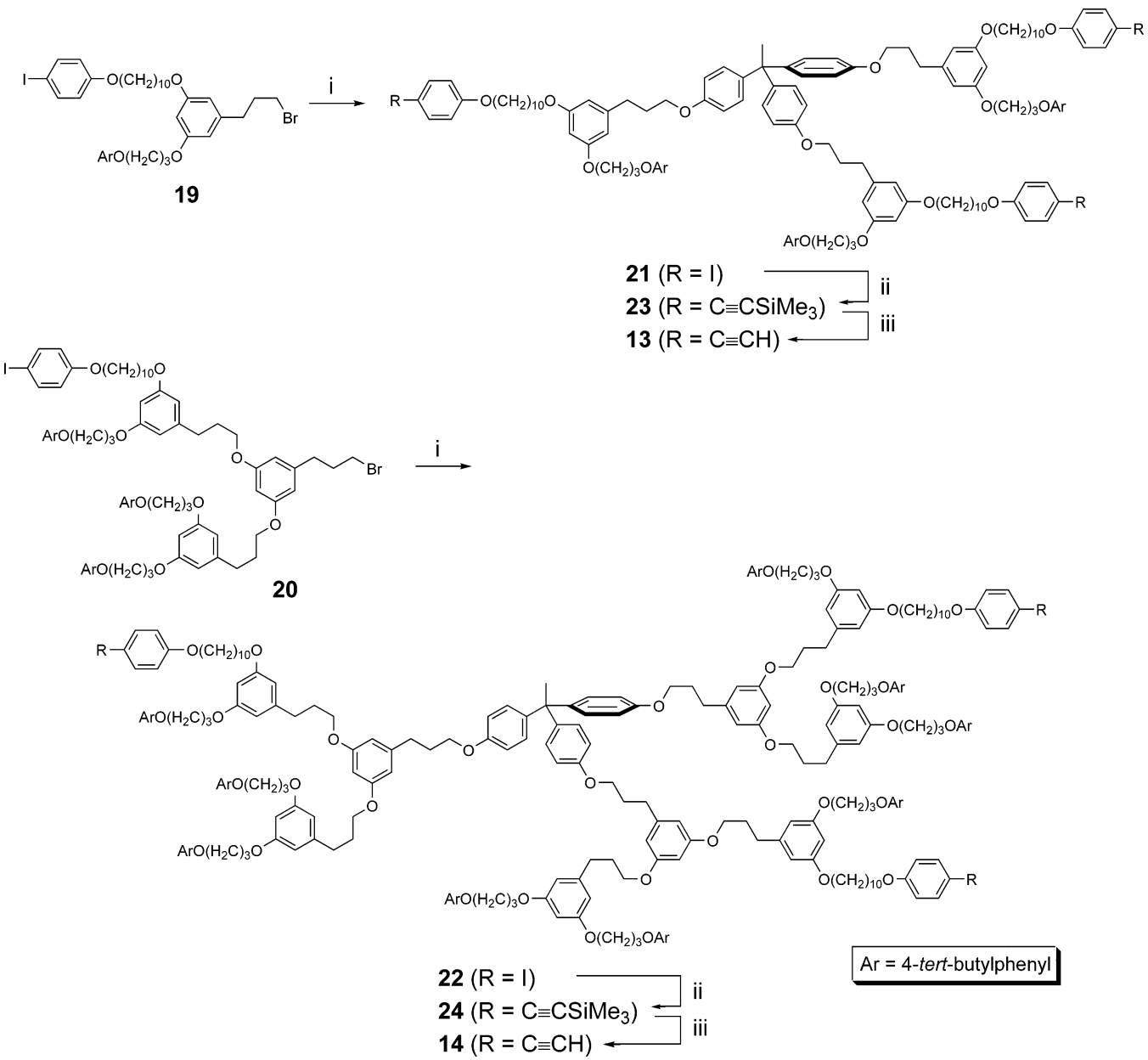

[a] Reagents and conditions: (i) 1,1,1-tris(4-hydroxyphenyl)ethane (**16**) (0.31 equiv), Cs_2CO_3, dibenzo-24-crown-8, DMF, 110 °C, 2 h; (ii) $(CH_3)_3SiC{\equiv}CH$, $Pd(PPh_3)_2Cl_2$, CuI, PPh_3, NEt_3, toluene, 60 °C, 6 h; (iii) K_2CO_3, MeOH, THF, 25 °C, 1.5 h.

Scheme 6[a]

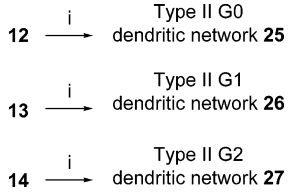

[a] Reagents and conditions: (i) **5** (1.5 equiv), CuI (catalytic), CH_2Cl_2/*i*-Pr_2NH (1:1), 25 °C, 12 h.

The molecular weights of the dendritic species were determined by mass spectroscopic analysis. Apart from the triiodo G2 **22** and tris(ethynyl) G2 **14** surface-functionalized dendrimers, all compounds gave a molecular peak corresponded to the theoretical value in their respective mass spectrum. In addition to mass spectroscopic analysis, SEC was also used to estimate the molecular weights and purity of the synthesized compounds (Table 3). All compounds gave a sharp peak with a PDI value of 1.02−1.03, confirming the good homogeneity of the compounds. The GPC estimated molecular weight values (M_w), however, were slightly higher than their corresponding to theoretical values (M_{calcd}).

The insoluble type II networks were examined by EDX spectroscopy to determine their elemental compositions (Table 4). The decreasing trend of the % Pt and % P contents and the increasing trend of the % C content with increasing dendrimer generation were clearly noted. As expected, the measured elemental compositions deviated from the calculated values, but the discrepancies were in line with the accuracy of this technique.

Dried gels of the type II insoluble organoplatinum dendritic networks **12**−**14** were visualized by SEM technique (Figure 8). All images showed the presence of highly dense structures that were consistent with their highly cross-linking architecture. In addition, the

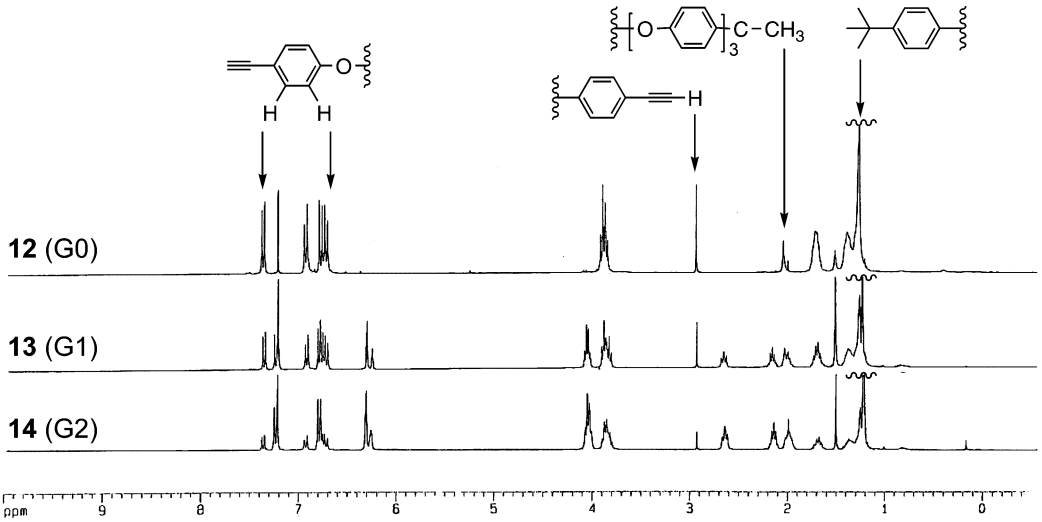

Figure 7. ^{1}H (300 MHz, $CDCl_3$) nuclear magnetic resonance spectra of tris(ethynyl) surface-functionalized dendritic monomers **12**−**14**.

Table 3. Size Exclusion Chromatography Data of G1−G3 Dendritic Molecules[a]

compound	M_{calcd}[b] (g/mol)	M_w[c] × 10^{-3} (g/mol)	PDI[d]
17	1381	1.4	1.02
18	1292	1.3	1.02
12	1076	1.2	1.03
21	2403	2.7	1.02
23	2313	2.6	1.02
13	2097	2.3	1.03
22	4445	6.2	1.03
24	4356	5.9	1.03
14	4140	5.1	1.03

[a] Columns: Waters Styragel columns HR 1, HR 2, HR 3, and HR 4 in series. Solvent: THF (flow rate = 1.0 mL/min). Temperature: 40 °C. Calibration standards: polystyrenes. [b] M_{calcd}= calculated theoretical molecular weight. [c] M_w = weight-average molecular weight. [d] PDI = polydispersity index M_w/M_n.

Table 4. Energy Dispersive X-ray Analysis Results of the Type II Dendritic Networks 12−14[a]

dendritic network	elemental content (%)[a]		
	Pt	C	P
G0 **12**	26.7 (21.9, 18.3)	55.1 (60.3, 64.1)	5.3 (7.0, 5.8)
G1 **13**	24.2 (15.9, 12.4)	62.1 (65.1, 68.5)	4.5 (5.0, 3.9)
G2 **14**	17.9 (10.2, 7.5)	66.4 (69.6, 72.1)	3.6 (3.2, 2.4)

[a] First and second values in parentheses are theoretical values calculated from molecular structures with perfect branching pattern and from 1:1 linear structures without branching, respectively.

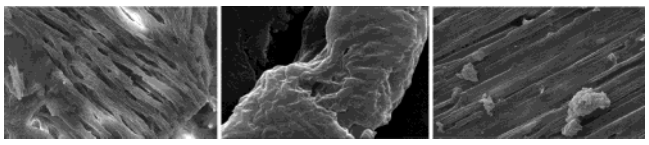

Figure 8. Scanning electron microscopy images (dried gels) of type II G0 (left: 80 μm × 50 μm), G1 (middle: 10 μm × 6.5 μm), and G2 (right: 100 μm × 65 μm) networks.

G0 **12** and G2 **14** images consisted of long thick threadlike filaments (cross sectional diameter ~ 3 μm) that were aligned in parallel with respect to each other.

3. Conclusions

This paper examines two different protocols toward the syntheses of highly cross-linking dendritic networks from simple dendritic monomers using an outer sphere−outer sphere connection strategy. In our first approach, bis(ethynyl) surface-functionalized dendritic monomers **6**−**8** were copolymerized with a small size trifunctional organoplatinum brancher **3** to form type I dendritic networks **9**−**11**, respectively. It was found that the steric size of the dendritic components had a profound effect on the cross-linking efficiency. Only in the copolymerization of the smallest size G1 dendritic monomer **6** with the organoplatinum brancher **3** could lead to the formation of a dendritic network, while the copolymerizations of the larger G2 **7** and G3 **8** dendritic monomers with brancher **3** produced linear dendritic necklaces with little cross-linking. In our second approach, a small size bifunctional organoplatinum monomer **5** was copolymerized with various tris(ethynyl) surface-functionalized dendrimers **12**−**14** to produce type II dendritic networks **25**−**27**, respectively. In contrast to the first protocol, the size of the dendritic components had little effect on the cross-linking efficiency; dendritic gels were formed with all three generation of dendritic monomers. Therefore, highly cross-linking dendritic networks could be efficiently synthesized when the reactive surface functional groups on the branching monomers were far apart. The difference in the copolymerization behavior of the two protocols could be rationalized in terms of steric crowding around the vicinity of the branching point in the type I dendritic architecture. More interestingly, the preferential formation of linear dendritic polymers instead of highly cross-linking dendritic networks from the outer sphere−outer sphere copolymerization between bulky bifunctional dendritic monomers and small trifunctional comonomers was not commonly observed in copolymerization reactions involving small size monomers and comonomers. Although further addition of bulky monomers to the branching points of the above linear dendritic polymers appears difficult, however, this process may become feasible for smaller size functional molecules and hence one may use this strategy to prepare novel linear functional dendritic polymers containing multiple functionalities at each potential branching junctures.

4. Experimental Section

4.1. Materials. 1,1,1-tris(4-hydroxyphenyl)ethane (**16**) (99%), Cs_2CO_3 (99.9%), $Pd(PPh_3)_2Cl_2$ (99.99%), PPh_3 (99%), *trans*-[$Pt(PEt_3)_2Cl_2$] (98%), CuI (99.999%), and CuCl (>99%) were

purchased from Aldrich and trimethylsilylacetylene (98%) was obtained from Acros. The bis(ethynyl) surface-functionalized G1−G3 dendrimers **6**−**8** and the G0−G2 bromide dendrons **15**, **19**, and **20** (all of purity ≥95%) were prepared according to literature procedures.[6] The trifunctional branching organoplatinum complex **3** (purity ≥98%) was synthesized according to the literature[9] reported by Takahashi. 1,1′-Bis(ethynyl)-4,4′-biphenyl (purity ≥98%) was prepared according to the procedure[10] described by Hagihara. All reaction solvents were distilled before use.

4.2. Instrumentation. Nuclear magnetic resonance (NMR) spectra were recorded either on a Brüker Avance DPX300 (^{1}H, 300 MHz; ^{13}C, 75.5 MHz) or a Varian Unity INOVA400 spectrometer (^{31}P, 161.9 MHz) and chloroform-*d* was used as the solvent unless otherwise stated. Chemical shifts are reported as parts per million on the δ scale using the signal of chloroform as an internal standard for ^{1}H and ^{13}C NMR and the signal of PPh_3 as an external standard for ^{31}P NMR spectroscopy. Coupling constants (*J*) are reported in hertz (Hz). For ^{1}H and ^{13}C NMR spectral assignments, the resonated nuclei are highlighted in italics in the structural formula. Mass spectra were obtained by fast atom bombardment (FAB) on a Hewlett-Packard 5989B mass spectrometer or matrix-assisted laser desorption/ionization time-of-flight mass spectrometry (MALDI−TOF) on a Brüker Biflex TOF mass spectrometer. The reported molecular mass (*m*/*z*) values are the most abundant monoisotopic mass. Elemental analyses were carried out at MEDAC Ltd. (Egham, Surrey, UK). Size exclusion chromatography (SEC) analyses were performed on Waters Styragel columns [HR 1 (effective molecular weight range (EMWR): 100−5000), HR 2 (EMWR: 500−20 000), HR 3 (EMWR: 500−30 000), and HR 4 (EMWR: 5000−500 000) in series] at 40 °C using THF as eluent (flow rate = 1.0 mL/min) on a Waters HPLC 515 pump equipped with a Waters 486 tunable UV absorbance detector. Molecular weights obtained from SEC measurements were based on a calibration curve derived from polystyrene standards. Melting points were measured on an Electrothermal 9100 digital melting point apparatus and are uncorrected. Scanning electron microscopy was performed with a Leo 1450 VP scanning electron microscope at an accelerating voltage of 20 keV, and the energy-dispersive X-ray spectroscopic data were recorded using an Oxford INCA detector. The dried polymer gels were coated with a gold layer using a Polaron SC502 sputter coater. Scanning tunneling microscopic experiments were conducted on an Omicron UHV AFM/STM instrument at a gap voltage of 0.1−0.3 V and feedback current at 0.2−0.5 nA. Samples were prepared by spin-coating of a solution of the polymer samples at 2000 rpm on HOPG and then heated at 40 °C in air for 1 h.

4.3. Synthesis. 4.3.1. General Information. All reactions were conducted under N_2 atmosphere unless otherwise stated. R_f values of synthesized compounds were obtained from thin-layer chromatography (TLC) performed on silica gel sheets 60 F_{254} (E. Merck). Column chromatography was performed on silica gel (Macherey Nagel Kieselgel 60 M 230−400 mesh).

4.3.2. Synthesis of Surface Trifunctionalized Dendrimers. Triiodo G0 Dendrimer 17. A mixture of 1,1,1-tris(4-hydroxyphenyl)ethane (**16**) (0.33 g, 1.1 mmol), the G0 bromide dendron **15** (1.50 g, 3.4 mmol), Cs_2CO_3 (1.70 g, 5.3 mmol), and dibenzo-24-crown-8 (0.30 g, 0.53 mmol) in DMF (12 mL) was heated at 110 °C for 2 h. The reaction was then quenched with water and extracted with EtOAc (25 mL × 2). The organic layers were combined, washed with brine (25 mL), dried ($MgSO_4$) and concentrated under reduced pressure. The residue was purified by column chromatography (eluent: hexane gradient to hexane/EtOAc = 8/1) to afford compound **17** (0.70 g, 47%) as a colorless oil. R_f: 0.62 (hexane/EtOAc = 5/1). ^{1}H NMR: 1.25−1.50 (m, 36 H), 1.76 (quin, J = 6.0, 12 H), 2.10 (s, 3 H, Ar_3CCH_3), 3.91 (t, J = 6.3, 6 H, $ArOCH_2$), 3.93 (t, J = 6.3, 6 H, $ArOCH_2$), 6.66 (d, J = 6.9, 6 H, Ar*H*), 6.77 (d, J = 6.9, 6 H, Ar*H*), 6.98 (d, J = 8.7, 6 H, Ar*H*), 7.53 (d, J = 8.7, 6 H, Ar*H*). ^{13}C NMR: 25.9, 26.1, 29.1, 29.3, 29.4, 30.8, 50.5 (Ar_3CMe), 67.8, 68.1, 82.4 (*C*−I), 113.5, 116.9, 129.6, 138.1, 141.6, 157.1, 159.0. SEC: R_t 31.33 min. MS (FAB): *m*/*z* 1381 (M^+, 15%). Anal. Calcd for $C_{68}H_{87}O_6I_3$: C, 59.14; H, 6.35. Found: C, 58.79; H, 6.43.

Triiodo G1 Dendrimer 21. A mixture of 1,1,1-tris(4-hydroxyphenyl)ethane (**16**) (0.11 g, 0.36 mmol), the G1 bromide dendron **19** (0.90 g, 1.2 mmol), Cs_2CO_3 (0.60 g, 1.8 mmol), and dibenzo-24-crown-8 (80 mg, 0.18 mmol) in DMF (8 mL) was heated at 110 °C for 2 h. The reaction was quenched with water and extracted with EtOAc (25 mL × 2). The organic layers were combined, washed with brine (25 mL), dried ($MgSO_4$), and concentrated under reduced pressure. The residue was then purified by column chromatography (eluent: hexane/EtOAc = 10/1 gradient to 8/1) to give compound **21** (0.41 g, 47%) as a colorless oil. R_f: 0.48 (hexane/EtOAc = 5/1). ^{1}H NMR: 1.25−1.50 (m, 36 H), 1.29 (s, 27 H, $C(CH_3)_3$), 1.65−1.80 (m, 12 H), 2.05−2.10 (m, 9 H, Ar_3CCH_3 and $ArCH_2CH_2CH_2O$), 2.21 (quin, J = 6.0, 6 H, $OCH_2CH_2CH_2O$), 2.72 (t, J = 6.4, 6 H, $ArCH_2$), 3.85−4.00 (m, 18 H, $ArOCH_2$), 4.10 (t, J = 5.7, 6 H, $ArOCH_2$), 4.12 (t, J = 5.7, 6 H, $ArOCH_2$), 6.31 (t, J = 2.1, 3 H, Ar*H*), 6.36 (d, J = 1.8, 6 H, Ar*H*), 6.66 (d, J = 9.0, 6 H, Ar*H*), 6.78 (d, J = 8.7, 6 H, Ar*H*), 6.85 (d, J = 6.9, 6 H, Ar*H*), 6.98 (d, J = 8.7, 6 H, Ar*H*), 7.29 (d, J = 8.7, 6 H, Ar*H*), 7.53 (d, J = 8.7, 6 H, Ar*H*). ^{13}C NMR: 25.96, 26.04, 29.1, 29.4, 29.5, 30.7, 31.5 ($C(CH_3)_3$), 32.5, 34.0, 50.6 (Ar_3CMe), 64.36, 64.43, 66.9, 67.9, 68.1, 82.4 (*C*−I), 98.8, 106.9, 107.3, 113.6, 113.9, 116.9, 126.2, 129.6, 138.1, 141.7, 143.4, 143.9, 156.6, 157.0, 159.0, 160.0, 160.3. SEC: R_t 29.45 min. MS (MALDI−TOF): *m*/*z* 2423.9 [$(M+Na)^+$, 22%]. Anal. Calcd for $C_{134}H_{171}O_{15}I_3$: C, 66.99; H, 7.17. Found: C, 67.32; H, 7.35.

Triiodo G2 Dendrimer 22. A mixture of 1,1,1-tris(4-hydroxyphenyl)ethane (**16**) (44 mg, 0.14 mmol), the G2 bromide dendron **20** (0.66 g, 0.45 mmol), Cs_2CO_3 (0.23 g, 0.71 mmol) and dibenzo-24-crown-8 (32 mg, 0.07 mmol) in DMF (4 mL) was heated at 110 °C for 2 h. The reaction was then quenched with water and extracted with EtOAc (25 mL × 2). The organic layers were combined, washed with brine (25 mL), dried ($MgSO_4$) and concentrated under reduced pressure. The residue was then purified by column chromatography (eluent: hexane/EtOAc = 5/1) to produce compound **22** (0.23 g, 36%) as a colorless oil. R_f: 0.51 (hexane/EtOAc = 3/1). ^{1}H NMR: 1.25−1.50 (m, 36 H), 1.29 (s, 81 H, $C(CH_3)_3$), 1.70−1.80 (m, 12 H), 2.00−2.15 (m, 21 H, Ar_3CCH_3 and $ArCH_2CH_2CH_2O$), 2.15−2.25 (m, 18 H, $OCH_2CH_2CH_2O$), 2.70 (t, J = 6.9, 18 H, $ArCH_2$), 3.84−4.00 (m, 30 H, $ArOCH_2$), 4.09 (t, J = 5.7, 18 H, $ArOCH_2$), 4.10 (t, J = 5.7, 18 H, $ArOCH_2$), 6.25−6.40 (m, 27 H, Ar*H*), 6.65 (d, J = 8.7, 6 H, Ar*H*), 6.77 (d, J = 8.7, 6 H, Ar*H*), 6.84 (d, J = 8.7, 18 H, Ar*H*), 6.97 (d, J = 9.0, 6 H, Ar*H*), 7.28 (d, J = 9.0, 18 H, Ar*H*), 7.52 (d, J = 6.9, 6 H, Ar*H*). ^{13}C NMR (signal of the quaternary carbon of the central core was too weak to be detected): 26.0, 29.1, 29.4, 29.5, 30.7, 30.8, 31.5 ($C(CH_3)_3$), 32.5, 34.0, 64.36, 64.44, 66.9, 67.9, 68.1, 82.4 (*C*−I), 98.9, 107.1, 107.2, 113.6, 113.9, 116.9, 126.2, 129.6, 138.1, 141.7, 143.3, 143.9, 144.0, 156.6, 157.0, 159.0, 160.0, 160.2, 160.3. SEC: R_t 27.43 min. Anal. Calcd for $C_{266}H_{339}O_{33}I_3$: C, 71.87; H, 7.69. Found: C, 72.20; H, 7.62.

Tris(trimethylsilylethynyl) G0 Dendrimer 18. A mixture of the triiodo G0 dendrimer **17** (0.60 g, 0.43 mmol), trimethylsilylacetylene (0.60 mL, 4.3 mmol), CuI (10 mg, 0.053 mmol), PPh_3 (10 mg, 0.038 mmol), $Pd(PPh_3)_2Cl_2$ (60 mg, 0.085 mmol), and NEt_3 (0.6 mL) in toluene (8 mL) was stirred in a sealed tube at 60 °C for 6 h. The mixture was filtered and washed with Et_2O (20 mL). The filtrate obtained was concentrated under reduced pressure and the residue purified by column chromatography (eluent: hexane gradient to hexane/EtOAc = 10/1) to afford compound **18** (0.50 g, 89%) as a yellow oil. R_f: 0.74 (hexane/EtOAc = 5/1). ^{1}H NMR: 0.24 (s, 27 H, $Si(CH_3)_3$), 1.25−1.50 (m, 36 H), 1.76 (quin, J = 6.6, 12 H), 2.10 (s, 3 H, Ar_3CCH_3), 3.92 (t, J = 6.3, 6 H, $ArOCH_2$), 3.94 (t, J = 6.3, 6 H, $ArOCH_2$), 6.77 (d, J = 6.0, 6 H, Ar*H*), 6.80 (d, J = 6.0, 6 H, Ar*H*), 6.98 (d, J = 8.7, 6 H, Ar*H*), 7.39 (d, J = 8.7, 6 H, Ar*H*). ^{13}C NMR: 0.1 ($Si(CH_3)_3$), 26.0, 26.1, 29.2, 29.3, 29.5, 30.8, 50.5 (Ar_3CMe), 67.8, 68.0, 92.3 (C≡*C*Si), 105.3 (Ar*C*≡C), 113.5, 114.3, 114.9, 129.6, 133.4, 141.7, 157.1, 159.3. SEC: R_t 31.40 min. MS (FAB): *m*/*z* 1292 (M^+, 12%). Anal. Calcd for $C_{83}H_{114}O_6Si_3$: C, 77.16; H, 8.89. Found: C, 76.72; H, 9.18.

Tris(trimethylsilylethynyl) G1 Dendrimer 23. A mixture of the triiodo G1 dendrimer **21** (0.40 g, 0.17 mmol), trimethylsilylacetylene (0.30 mL, 2.1 mmol), CuI (2 mg, 0.01 mmol), PPh_3 (2 mg, 0.008 mmol), $Pd(PPh_3)_2Cl_2$ (20 mg, 0.028 mmol), and NEt_3 (0.3 mL) in toluene (4 mL) was stirred in a sealed tube at 60 °C for 6 h. The mixture was filtered and then washed with Et_2O (20 mL). The filtrate obtained was concentrated under reduced pressure. The residue was purified by column chromatography (eluent: hexane gradient to hexane/EtOAc = 10/1) to give compound **23** (0.30 g, 78%) as a yellow oil. R_f: 0.44 (hexane/EtOAc = 5/1). ^{1}H NMR: 0.23 (s, 27 H, $Si(CH_3)_3$), 1.25−1.50 (m, 36 H), 1.29 (s, 27 H, $C(CH_3)_3$) 1.75−1.80 (m, 12 H), 2.05−2.10 (m, 9 H, Ar_3CCH_3 and $ArCH_2CH_2CH_2O$), 2.21 (quin, J = 6.0, 6 H, $OCH_2CH_2CH_2O$), 2.72 (t, J = 6.4, 6 H, $ArCH_2$), 3.85−4.00 (m, 18 H, $ArOCH_2$), 4.11 (t, J = 5.4, 6 H, $ArOCH_2$), 4.12 (t, J = 5.4, 6 H, $ArOCH_2$), 6.30 (t, J = 2.1, 3 H, Ar*H*), 6.36 (d, J = 1.8, 6 H, Ar*H*), 6.72−6.87 (m, 18 H, Ar*H*), 6.97 (d, J = 9.0, 6 H, Ar*H*), 7.28 (d, J = 8.7, 6 H, Ar*H*), 7.38 (d, J = 8.7, 6 H, Ar*H*). ^{13}C NMR: 0.1 ($Si(CH_3)_3$), 26.0, 29.2, 29.4, 29.5, 30.7, 31.5 ($C(CH_3)_3$), 32.5, 34.0, 50.6 (Ar_3CMe), 64.35, 64.42, 66.9, 67.9, 68.0, 92.2 (C≡CSi), 98.8, 105.3 (ArC≡C), 106.9, 107.2, 113.6, 113.9, 114.3, 126.2, 129.6, 133.4, 141.7, 143.4, 143.9, 156.6, 157.0, 159.3, 160.0, 160.3. SEC: R_t 29.06 min. MS (MALDI−TOF): m/z 2337.1 [(M + Na)$^+$, 100%]. Anal. Calcd for $C_{149}H_{198}O_{15}Si_3$: C, 77.36; H, 8.63. Found: C, 77.37; H, 8.62.

Tris(trimethylsilylethynyl) G2 Dendrimer 24. A mixture of the triiodo G2 dendrimer **22** (0.23 g, 0.052 mmol), trimethylsilylacetylene (0.10 mL, 0.71 mmol), CuI (2 mg, 0.01 mmol), PPh_3 (2 mg, 0.008 mmol), $Pd(PPh_3)_2Cl_2$ (10 mg, 0.014 mmol), and NEt_3 (0.10 mL) in toluene (1 mL) was stirred in a sealed tube at 60 °C for 6 h. The mixture was filtered and washed with Et_2O (20 mL). The filtrate was concentrated under reduced pressure and the residue was purified by column chromatography (eluent: hexane gradient to hexane/EtOAc = 5/1) to afford compound **24** (0.15 g, 67%) as a yellow oil. R_f: 0.71 (hexane/EtOAc = 3/1). ^{1}H NMR: 0.23 (s, 27 H, $Si(CH_3)_3$), 1.25−1.50 (m, 36 H), 1.28 (s, 81 H, $C(CH_3)_3$), 1.65−1.80 (m, 12 H), 2.05−2.10 (m, 21 H, Ar_3CCH_3 and $ArCH_2CH_2CH_2O$), 2.20 (quin, J = 5.7, 18 H, $OCH_2CH_2CH_2O$), 2.70 (t, J = 7.2, 18 H, $ArCH_2$), 3.84−4.00 (m, 30 H, $ArOCH_2$), 4.08 (t, J = 7.5, 18 H, $ArOCH_2$), 4.10 (t, J = 7.5, 18 H, $ArOCH_2$), 6.27−6.37 (m, 27 H, Ar*H*), 6.73−6.86 (m, 30 H, Ar*H*), 6.97 (d, J = 9.0, 6 H, Ar*H*), 7.28 (d, J = 8.7, 18 H, Ar*H*), 7.38 (d, J = 8.7, 6 H, Ar*H*). ^{13}C NMR (signals of C≡C and the quaternary carbon of the central core were too weak to be detected): 0.1 ($Si(CH_3)_3$), 26.0, 29.2, 29.4, 29.5, 30.7, 31.5 ($C(CH_3)_3$), 32.5, 34.0, 64.35, 64.43, 66.9, 68.0, 98.8, 107.1, 107.2, 113.6, 113.9, 114.3, 126.2, 129.6, 133.4, 143.3, 143.8, 156.6, 160.0, 160.2. SEC: R_t 27.83 min. MS (MALDI−TOF): m/z 4378.3 [(M + Na)$^+$, 8%]. Anal. Calcd (%) for $C_{281}H_{366}O_{33}Si_3$: C, 77.48; H, 8.47. Found: C, 77.05; H, 8.27.

Tris(ethynyl) G0 Dendrimer 12. Powdered K_2CO_3 (0.33 g, 2.4 mmol) was added into a solution of the tris(trimethylsilylethynyl) G0 dendrimer **18** (0.50 g, 0.39 mmol) in MeOH/THF (1:1, 4 mL). The mixture was stirred at 25 °C for 1.5 h. The reaction was then quenched with water and extracted with EtOAc (50 mL × 2). The combined organic layers were washed with brine (50 mL), dried ($MgSO_4$), and concentrated under reduced pressure. The residue was purified by column chromatography (eluent: hexane/EtOAc = 8/1) to afford compound **12** (0.23 g, 55%) as a colorless oil. R_f: 0.51 (hexane/EtOAc = 5/1). ^{1}H NMR: 1.20−1.50 (m, 36 H), 1.70−1.85 (m, 12 H), 2.10 (s, 3 H, Ar_3CCH_3), 2.99 (s, 3 H, C≡CH), 3.92 (t, J = 6.6, 6 H, $ArOCH_2$), 3.94 (t, J = 6.6, 6 H, $ArOCH_2$), 6.78 (d, J = 7.8, 6 H, Ar*H*), 6.82 (d, J = 7.8, 6 H, Ar*H*), 6.98 (d, J = 8.7, 6 H, Ar*H*), 7.41 (d, J = 8.7, 6 H, Ar*H*). ^{13}C NMR: 26.0, 26.1, 29.1, 29.3, 29.5, 30.8, 50.5 (Ar_3CMe), 67.8, 68.0, 75.6 (C≡CH), 83.8 (ArC≡C), 113.5, 113.8, 114.4, 129.6, 133.5, 141.7, 157.1, 159.5. SEC: R_t 31.27 min. MS (FAB): m/z 1076 (M$^+$, 14%). Anal. Calcd for $C_{74}H_{90}O_6$: C, 82.64; H, 8.43. Found: C, 82.59; H, 8.57.

Tris(ethynyl) G1 Dendrimer 13. Powdered K_2CO_3 (0.20 g, 1.5 mmol) was added into a solution of the tris(trimethylsilylethynyl) G1 dendrimer **23** (0.30 g, 0.13 mmol) in MeOH/THF (1:1, 3 mL). The mixture was stirred at 25 °C for 1.5 h. The reaction was then quenched with water and extracted with EtOAc (40 mL × 2). The combined organic layers were washed with brine (40 mL), dried ($MgSO_4$), and concentrated under reduced pressure. The residue was purified by column chromatography (eluent: hexane/EtOAc = 8/1 gradient to 5/1) to afford compound **13** (0.20 g, 74%) as a colorless oil. R_f: 0.37 (hexane/EtOAc = 5/1). ^{1}H NMR: 1.25−1.50 (m, 36 H), 1.29 (s, 27 H, $C(CH_3)_3$), 1.75−1.80 (m, 12 H), 2.05−2.10 (m, 9 H, Ar_3CCH_3 and $ArCH_2CH_2CH_2O$), 2.21 (quin, J = 6.0, 6 H, $OCH_2CH_2CH_2O$), 2.72 (t, J = 6.4, 6 H, $ArCH_2$), 2.98 (s, 3 H, C≡CH), 3.85−4.00 (m, 18 H, $ArOCH_2$), 4.10 (t, J = 5.4, 6 H, $ArOCH_2$), 4.11 (t, J = 5.4, 6 H, $ArOCH_2$), 6.30 (t, J = 2.1, 3 H, Ar*H*), 6.35 (d, J = 1.8, 6 H, Ar*H*), 6.74−6.88 (m, 18 H, Ar*H*), 6.97 (d, J = 9.0, 6 H, Ar*H*), 7.28 (d, J = 8.7, 6 H, Ar*H*), 7.40 (d, J = 8.7, 6 H, Ar*H*). ^{13}C NMR: 25.97, 26.04, 29.1, 29.28, 29.35, 29.5, 30.7, 30.8, 31.5 ($C(CH_3)_3$), 32.5, 34.0, 50.6 (Ar_3CMe), 64.35, 64.42, 66.9, 67.9, 68.0, 75.6 (C≡CH), 83.8 (ArC≡C), 98.8, 106.9, 107.2, 113.6, 113.8, 113.9, 114.4, 126.2, 129.6, 133.5, 141.7, 143.4, 143.9, 156.6, 157.0, 159.5, 160.0, 160.3. SEC: R_t 29.26 min. MS (MALDI−TOF): m/z 2118.4 [(M + Na)$^+$, 12%]. Anal. Calcd for $C_{140}H_{174}O_{15}$: C, 80.19; H, 8.36. Found: C, 80.32; H, 8.47.

Tris(ethynyl) G2 Dendrimer 14. Powdered K_2CO_3 (50 mg, 0.36 mmol) was added into a solution of the tris(trimethylsilylethynyl) G2 dendrimer **24** (0.15 g, 0.034 mmol) in MeOH/THF (1:1, 2 mL). The mixture was stirred at 25 °C for 1.5 h. The reaction was then quenched with water and extracted with EtOAc (30 mL × 2). The combined organic layers were washed with brine (30 mL), dried ($MgSO_4$), and concentrated under reduced pressure. The residue was purified by column chromatography (eluent: hexane/EtOAc = 6/1) to give compound **14** (0.12 g, 84%) as a colorless oil. R_f: 0.43 (hexane/EtOAc = 3/1). ^{1}H NMR: 1.25−1.50 (m, 36 H), 1.28 (s, 81 H, $C(CH_3)_3$), 1.65−1.80 (m, 12 H), 2.05−2.10 (m, 21 H, Ar_3CCH_3 and $ArCH_2CH_2CH_2O$), 2.20 (quin, J = 6.0, 18 H, $OCH_2CH_2CH_2O$), 2.70 (t, J = 7.5, 18 H, $ArCH_2$), 2.98 (s, 3 H, C≡CH), 3.84−4.00 (m, 30 H, $ArOCH_2$), 4.08 (t, J = 7.5, 18 H, $ArOCH_2$), 4.10 (t, J = 7.5, 18 H, $ArOCH_2$), 6.30−6.40 (m, 27 H, Ar*H*), 6.74−6.87 (m, 30 H, Ar*H*), 6.97 (d, J = 8.7, 6 H, Ar*H*), 7.28 (d, J = 8.7, 18 H, Ar*H*), 7.40 (d, J = 8.7, 6 H, Ar*H*). ^{13}C NMR (signal of the quaternary carbon of the central core was too weak to be detected): 26.0, 29.1, 29.4, 29.5, 30.7, 31.5 ($C(CH_3)_3$), 32.5, 34.0, 64.35, 64.44, 66.9, 67.9, 68.0, 75.6 (C≡CH), 83.8 (ArC≡C), 98.9, 107.1, 107.2, 113.6, 113.9, 114.4, 126.2, 129.6, 133.5, 141.7, 143.3, 143.9, 156.6, 157.0, 159.5, 160.0, 160.2. SEC: R_t 28.28 min. Anal. Calcd for $C_{272}H_{342}O_{33}$: C, 78.92; H, 8.33. Found: C, 78.78; H, 8.24.

4.3.3. Diplatinum Complex 5. A mixture of 1,1′-bis(ethynyl)-4,4′-biphenyl (0.35 g, 1.7 mmol), *trans*-$[Pt(PEt_3)_2Cl_2]$ (1.90 g, 3.78 mmol) and CuCl (40 mg, 0.40 mmol) in *i*-Pr_2NH/PhMe (1:1, 20 mL) was heated at 100 °C for 6 h. The excess solvent was then evaporated under reduced pressure and the residue purified by column chromatography (eluent: hexane/EtOAc = 4/1) to give the diplatinum complex **5** (1.00 g, 51%) as a yellow solid. R_f: 0.42 (hexane/EtOAc = 3/1). Mp > 230 °C dec. ^{1}H NMR: 1.21 (dt, J = 16.2 and 7.8, 36 H, PCH_2CH_3), 2.00−2.20 (m, 24 H, PCH_2CH_3), 7.29 (d, J = 8.1, 4 H, Ar*H*), 7.43 (d, J = 8.1, 4 H, Ar*H*). ^{13}C NMR: 8.0 (pseudo t, J = 9.7, PCH_2CH_3), 14.5 (pseudo quin, J = 17.1, PCH_2CH_3), 83.4 (t, J = 14.8), 101.5, 126.3, 127.5, 131.2, 137.7. ^{31}P{^{1}H} NMR: 17.51 ($^1J_{Pt-P}$ = 2393). MS (FAB): m/z 1133 (M$^+$, 52%). Anal. Calcd for $C_{40}H_{68}Cl_2P_4Pt_2$: C, 42.37; H, 6.04. Found: C, 42.32; H, 6.19.

4.3.4. Synthesis of Type I G1-G3 Dendritic Networks 9−11. Type I G1 Dendritic Network 9. A catalytic amount of CuI (5 mg, 0.03 mmol) was added to a mixture of the bis(ethynyl) G1 dendrimer **6** (0.123 g, 0.094 mmol), triplatinum complex **3** (0.10 g, 0.063 mmol) in CH_2Cl_2/*i*-Pr_2NH (1:1, 10 mL). After the reaction was stirred at 25 °C for 6 h, the excess solvent was evaporated under reduced pressure, and the resulting gel was washed with CH_2Cl_2 (10 mL). The resulting gel was broken up into small pieces and washed with CH_2Cl_2 to remove the soluble fractions. The sample was then freeze-dried to give the type I G1 dendritic network **9** (0.18 g, 83%) as a yellowish green solid.

Type I G2 Dendritic Network 10. A catalytic amount of CuI (9 mg, 0.05 mmol) was added to a mixture of the bis(ethynyl) G2 dendrimer **7** (0.40 g, 0.15 mmol) and triplatinum complex **3** (0.16 g, 0.10 mmol) in CH_2Cl_2/*i*-Pr_2NH (1:1, 20 mL). The mixture was stirred at 25 °C for 12 h. The solvent was evaporated under reduced pressure and the residue was redissolved in CH_2Cl_2 and then filtered through a short pad of alumina. The filtrate collected was concentrated under reduced pressure to about 1 mL and then added dropwise to an acetone solution (200 mL) to give the type I G2 dendritic network **10** (0.50 g, 90%) as a yellow solid. ^{1}H NMR: 1.10−1.25 (m, 46 H, PCH_2CH_3), 1.25−1.50 (m, 33 H), 1.28 (s, 54 H, $C(CH_3)_3$), 1.68−1.80 (m, 12 H), 1.97−2.25 (m, 58 H), 2.57 (s, ∼ 8 H, $ArCH_3$), 2.65−2.75 (m, 16 H, $ArCH_2$) 3.82−3.98 (m, 24 H, $ArCH_2O$), 4.08 (t, J = 7.2, 14 H, $ArCH_2O$), 4.10 (t, J = 7.2, 14 H, $ArCH_2O$), 6.28−6.32 (m, 6 H, Ar*H*), 6.32−6.38 (m, 12 H, Ar*H*), 6.73 (d, J = 8.7, 4 H, Ar*H*), 6.80 (s, 4 H, Ar*H*), 6.84 (d, J = 8.7, 12 H, Ar*H*), 7.21 (d, J = 8.7, 4 H, Ar*H*), 7.28 (d, J = 8.7, 12 H, Ar*H*). ^{13}C NMR (signals of the C≡C and the quaternary carbon of the central core were too weak to be detected): 8.4 (pseudo t, J = 9, PCH_2CH_3), 16.3 (pseudo quin, J = 17, PCH_2CH_3), 23.3, 26.1, 29.3, 30.7, 31.5, 32.5, 34.0, 64.3, 64.4, 66.9, 67.9, 98.9, 107.2, 113.9, 114.1, 115.4, 126.2, 132.0, 143.3, 143.9, 153.0, 156.6, 160.0, 160.2. ^{31}P{^{1}H} NMR: 15.13 ($^1J_{Pt-P}$ ∼ 2400), 17.81 ($^1J_{Pt-P}$ = 2393), 21.46 ($^1J_{Pt-P}$ ∼ 2400). UV: 275 nm (log ϵ = 4.1); 331 nm (log ϵ = 4.0).

Type I G3 Dendritic Network 11. A catalytic amount of CuI (2 mg, 0.01 mmol) was added to a mixture of the bis(ethynyl) G3 dendrimer **8** (0.20 g, 0.037 mmol), triplatinum complex **3** (40 mg, 0.025 mmol) in CH_2Cl_2/*i*-Pr_2NH (1:1, 10 mL). The mixture was stirred at 25 °C for 12 h. The solvent was evaporated under reduced pressure and the residue was redissolved in CH_2Cl_2 and then filtered through a short pad of alumina. The filtrate collected was concentrated under reduced pressure to about 1 mL and then added dropwise to an acetone solution (200 mL) to give the type I G3 dendritic network **11** (0.20 g, 84%) as a yellow precipitate. ^{1}H NMR: 1.10−1.25 (m, 37 H, PCH_2CH_3), 1.25−1.46 (m, 33 H), 1.28 (s, 126 H, $C(CH_3)_3$), 1.70−1.80 (m, 8 H), 1.95−2.26 (m, 80 H), 2.57 (s, ∼ 4 H, $ArCH_3$), 2.65−2.75 (m, 28 H, $ArCH_2$), 3.85−3.95 (m, 36 H, $ArCH_2O$), 4.08 (t, J = 6.3, 28 H, $ArCH_2O$), 4.10 (t, J = 6.3, 28 H, $ArCH_2O$), 6.29−6.33 (m, 14 H, Ar*H*), 6.29−6.38 (s, 28 H, Ar*H*), 6.71 (d, J = 8.7, 4 H, Ar*H*), 6.81 (s, 4 H, Ar*H*), 6.84 (d, J = 8.7, 28 H, Ar*H*), 7.20 (d, J = 8.7, 4 H, Ar*H*), 7.28 (d, J = 8.7, 28 H, Ar*H*). ^{13}C NMR (signals of the C≡C and the quaternary carbon of the central core were too weak to be detected): 8.4 (PCH_2CH_3), 16.3 (PCH_2CH_3), 29.3, 30.7, 31.5, 32.5, 34.0, 64.3, 64.4, 66.9, 68.0, 98.9, 107.2, 113.9, 115.4, 126.2, 132.0, 143.3, 143.9, 156.6, 160.0, 160.2. ^{31}P{^{1}H} NMR: 15.13 ($^1J_{Pt-P}$ ∼ 2400) 17.77 ($^1J_{Pt-P}$ = 2393). UV: 275 nm (log ϵ = 4.2); 332 nm (log ϵ = 3.8).

4.3.5. Synthesis of Type II G0—G2 Dendritic Networks 25—27. Type II G0 Dendritic Network 25. A mixture of the tris(ethynyl) G0 dendrimer **12** (0.20 g, 0.19 mmol), the diplatinum complex **5** (0.32 g, 0.28 mmol), and CuI (4 mg) in CH_2Cl_2/*i*-Pr_2NH (1:1, 6 mL) was stirred at 25 °C for 12 h. The resulting gel was washed with CH_2Cl_2 (20 mL) and broken up into small pieces. The solvents were evaporated using a freeze-drying apparatus to afford the insoluble organoplatinum type II G0 dendritic network **25** (0.37 g, 75%) as a yellow solid.

Type II G1 Dendritic Network 26. A mixture of the tris(ethynyl) G1 dendrimer **13** (0.18 g, 0.086 mmol), the diplatinum complex **5** (0.15 g, 0.13 mmol) and CuI (2 mg) in CH_2Cl_2/*i*-Pr_2NH (1:1, 3 mL) was stirred at 25 °C for 12 h. The resulting gel was washed with CH_2Cl_2 (20 mL) and broken up into small pieces. The solvents were then evaporated on a freeze-drying apparatus to give the insoluble type II G1 dendritic network **26** (0.26 g, 81%) as a yellow solid.

Type II G2 Dendritic Network 27. A mixture of the tris(ethynyl) G2 dendrimer **14** (0.12 g, 0.029 mmol), the diplatinum complex **5** (50 mg, 0.044 mmol) and CuI (1 mg) in CH_2Cl_2/*i*-Pr_2NH (1:1, 1 mL) was stirred at 25 °C for 12 h. The resulting gel was washed with CH_2Cl_2 (20 mL) and broken up into small pieces. The solvents were evaporated using a freeze-drying apparatus to produce the insoluble type II G2 dendritic network **27** (0.15 g, 90%) as a yellow solid.

Acknowledgment. We thank the Research Grants Council, HKSAR (CUHK4201/99P) for the financial support and Prof. D. W. T. Chan for mass measurements.

References and Notes

(1) Newkome, G. R.; Moorefield, C. N.; Vögtle, F. *Dendrimers and Dendrons. Concepts, Syntheses, Applications*; Wiley-VCH: Weinheim, Germany, 2001.
(2) (a) Schlüter, A. D.; Rabe, J. R. *Angew. Chem., Int. Ed.* **2000**, *39*, 864−883. (b) Zhang, A.; Shu, L.; Bo, Z.; Schlüter, A. D. *Macromol. Chem. Phys.* **2003**, *204*, 328−339.
(3) Percec, V.; Ahn, C.-H.; Ungar, G.; Yeardley, D. J. P.; Möller, M.; Sheiko, S. S. *Nature (London)* **1998**, *391*, 161−164.
(4) (a) Huck, W. T. S.; van Veggel, F. C. J. M.; Kropman, B. L.; Blank, D. H. A.; Keim, E. G.; Smithers, M. M. A.; Reinhoudt, D. N. *J. Am. Chem. Soc.* **1995**, *117*, 8293−8294. (b) Newkome, G. R.; He, E.; Godínez, L. A.; Baker, G. R. *J. Am. Chem. Soc.* **2000**, *122*, 9993−10006. (c) Gibson, H. W.; Yamaguchi, N.; Hamilton, L.; Jones, J. W. *J. Am. Chem. Soc.* **2002**, *124*, 4653−4665.
(5) (a) Watanabe, S.; Regen, S. L. *J. Am. Chem. Soc.* **1994**, *116*, 8855−8856. (b) Díaz, D. J.; Storrier, G. D.; Bernhard, S.; Takada, K.; Abruña, H. D. *Langmuir*, **1999**, *15*, 7351−7354.
(6) Chow, H.-F.; Leung, C.-F.; Li, W.; Wong, K.-W.; Xi, L. *Angew. Chem., Int. Ed.* **2003**, *42*, 4919−4923.
(7) For a review on linear polymers containing bis(alkynyl) platinum units on the main chain, see Hagihara, N.; Sonogashira, K.; Takahashi, S. *Adv. Polym. Sci.* **1981**, *41*, 149−179.
(8) Nondendritic, organoplatinum polymer networks of similar structural features had been reported, see Khan, M. S.; Schwartz, D. J.; Pasha, N. A.; Kakkar, A. K.; Lin, B.; Raithby, P. R.; Lewis, J. *Z. Anorg. Allg. Chem.* **1992**, *616*, 121−124.
(9) Ohshiro, N.; Takei, F.; Onitsuka, K.; Takahashi, S. *J. Organomet. Chem.* **1998**, *569*, 195−202.
(10) Takahashi, S.; Kuroyama, Y.; Sonogashira, K.; Hagihara, N. *Synthesis* **1980**, 627−630.

MA035548F